Reprinted from Preprint Volume. Seventh Symposium on Turbulence and Diffusion, November 12-15, 1985, Boulder, Colo. Published by the American Meteorological Society, Boston, Mass.

P2.3

MEASUREMENTS OF TWO-POINTS EULERIAN VELOCITY STATISTICS IN A TURBULENT BOUNDARY LAYER

Wen-Whai Li and Robert N. Meroney

Colorado State University
Fort Collins, Colorado 80523

1.0 INTRODUCTION

Turbulent flow has been described as an irregular fluid motion which is three-dimensional, continuous, diffusive and dissipative in nature. It forms such a complicated mathematical problem that its solution depends heavily on experimental data. A statistical approach to describe the mean motion of turbulent phenomenon seems to be most appropriate. The double velocity correlation function, namely the Eulerian space-time correlation, may be the most appropriate function to examine the structure of turbulence and its evolution in time (Townsend, 1976).

The double velocity correlation function is defined as

$$E^{R}_{ij}(\Delta x_1,\Delta x_2,\Delta x_3;\tau)=\frac{\overline{u_i(x_1,x_2,x_3;t)u_j(x_1+\Delta x_1,x_2+\Delta x_2,x_3+\Delta x_3;t+\tau)}}{[\overline{u_i^2(x_1,x_2,x_3;t)}]^{1/2}\ [\overline{u_j^2(x_1+\Delta x_1,x_2+\Delta x_2,x_3+\Delta x_3;t+\tau)}]^{1/2}}$$

where the overbar represents the Reynolds time average and u_i and u_j are the turbulent velocity components at their respective Eulerian locations, x_k

Pioneer correlation measurements of the space-time correlations in a turbulent flow were produced by Favre and his co-workers (1957, 1958, 1965, 1967). They performed measurements downstream of a grid, in a turbulent boundary layer and in a turbulent jet. Baldwin and his co-workers (1961, 1963) and Atesmen et al (1971) measured the space-time correlation in a fully developed turbulent pipe flow; while Blackwelder and Kovasznay (1972) reported correlation data for a turbulent boundary layer. Frenkiel and Klebnoff (1966) as well as Comte-Bellot and Corrsin (1971) reported space-time correlation measurements in a roughly isentropic grid-generated uniform flow. Champagne et al (1970) and later Harris et al (1977) extended the measurements to a nearly homogeneous turbulent uniform shear flow. Most of these researchers concentrated on the contribution of total turbulent energy from different sizes of eddy. Discussions were mostly focused on the statistical properties of turbulence, convective velocity and Taylor's hypothesis.

Little attention has been given to the integral scale and the implications of Eulerian space-time correlation. In this paper, Eulerian space-time correlations and associated integral scales obtained in a simulated atmospheric boundary layer with no longitudinal pressure gradient are examined. An universal formulation for the Eulerian space-time correlation is recommended.

Two TSI-1287 split film probes were employed in the present investigation of turbulence characteristics. All measurements were performed in the Meteorological Wind Tunnel (MWT) of the Fluid Dynamics and Diffusion Laboratory at Colorado State University. A detailed description of the MWT may be found in Plate and Cermak (1963). Experimental techniques and sources of error related to the correlation measurements are considered by Comte-Bellot and Corrsin (1970) and Li and Meroney (1985).

2.0 BOUNDARY LAYER CHARACTERISTICS

Figure 1 shows the mean velocity and the local turbulent intensity profiles over the wind-tunnel test section. Normalized data at different longitudinal stations in the test section are very similar. The variation with distance of the free stream velocity was found to be less than one percent with no trend to either increase or decrease; hence, homogeneity in the x_1-x_2 plane is preserved in the test boundary layer.

Counihan (1975) reviewed vast meteorological literature on fully developed adiabatic atmospheric boundary layers, and recommended some empirical formulae for atmospheric turbulence. The present boundary layer is compared in Table 1 with his regressive formulae based on a fixed roughness length. Wind tunnel results are within 30 percent deviation from his results, well within the variation in data he evaluated.

3.0 EULERIAN SPACE CORRELATION

Eulerian space correlations presented in this section include two f-type correlations and four g-type correlations according to Hinze's (1975) definition. Their integral scales are represented by L_{ij}, where i indicates the velocity component and j indicates the direction of spatial separation.

The longitudinal space correlation measurements, $E^{R}_{11}(\Delta x_1,0,x_3;0)$, are displayed in Figure 2. Figure 3 presents the space correlation of lateral velocity fluctuations, $E^{R}_{22}(0,\Delta x_2,x_3;0)$. The longitudinal correlation decays much slower than the lateral correlation which implies an elongation of turbulent eddies in the streamwise direction. Since both functions are f-type correlations $L_{11}/L_{22}=4.8$.

$R_{11}(0,\Delta x_2,x_3;0)$ and $R_{33}(0,\Delta x_2,x_3;0)$ are shown in Figures 4 and 5, respectively. The space correlation function increases as height increases and turbulence decreases in all cases. The other two g-type correlations with streamwise separations are plotted in Figures 6 and 7 Correlation with longitudinal separations seems to persist for a longer distance than correlation with transverse separations.

The corresponding integral length scales for all these space correlations are summarized in Table 2a. L_{11} is significantly larger than all other scales. A characteristic generally observed in the atmospheric boundary layer. Integral scales are normalized with L_{11} and compared to field observations (Teunissen, 1980) in Table 2b. Teunissen's measurements were made in a neutral-stable planetary boundary layer over typical rural terrain at a height of 11 m. The mean wind velocity in his measurements was about 9 m/sec. The turbulent intensities were 0.16, 0.11 and 0.07 for longitudinal, lateral and vertical direction, respectively. Hence, his field measurements are comparable to the present wind-tunnel measurements for $x_3/\delta = 0.044$. Teunissen's results confirm that the wind-tunnel boundary layer characterized the turbulence found in an atmospheric boundary layer.

4.0 EULERIAN SPACE-TIME CORRELATION

The longitudinal space-time correlation functions, (Li and Meroney, 1984) for filtered turbulence are reproduced in Figure 8. Each data point represents the peak of the individual cross-correlation observed at optimum delay time, τ_m, although τ_m may be different from the convective time $\Delta x_1/u$. Figure 9 displays $R_{11}(\Delta x_1,0,x_3;\Delta x_1/u)$ for unfiltered turbulence. The transverse space-time correlations, $R_{22}(\Delta x_1,0,x_3;\Delta x_1/u)$ and $R_{33}(\Delta x_1,0,x_3;\Delta x_1/u)$, are given in Figures 10 and 11. The space-time correlation function increases as height increases and $R_{11} > R_{22} > R_{33}$ for a given height.

Notice that the correlation function has a rapid drop at small times in Figure 8. Such a drop is more marked as the probe moves closer to the ground. Similar results have been observed in the atmosphere where probe wake effect appears unnoticeable (Lumley and Panofsky, 1964). One explanation for the drop would be that near the ground the turbulence level is stronger and small eddies become more dominant. The small eddies lose their correlation in a shorter time period which results in a decrease in the correlation as height decreases. Such effect is somehow diluted when large eddies are dominant in an unfiltered turbulent field.

The inadequacy of Taylor's frozen turbulence hypothesis is clearly seen in this turbulent boundary layer. According to Taylor's hypothesis, $R_{11}(\Delta x_1,0,x_3;\tau)$ should reach its maximum value of unity at a time $\tau = \Delta x_1/u$, but as a result of shear, the resultant higher level of turbulence and the small eddy behavior, the peak value of $R_{11}(\Delta x_1,0,x_3;\tau)$ can never regain its theoretical magnitude as observed in Figures 8 through 11. Even in a grid-generated turbulence examined by Frenkiel and Klebanoff (1966) and Comte-Bellot and Corrsin (1971), where the turbulence is not distorted by mean shear, large departures from a frozen pattern are observed.

Most investigators attribute the breakdown of Taylor's hypothesis to the loss of coherence of small eddies when downwind separations slowly exceed the larger eddy sizes. But data reported on the frequency filtered space-time correlation measurements by Favre et al (1957, 1958) suggest an equivalent breakdown in a boundary layer. Indeed, the turbulence gradually loses some coherence at the edge of the boundary layer where mean shear turbulence level are low, but near the ground the correlation function losses its identity quickly due to higher mean shear and turbulence levels.

Space time correlations measurements were extrapolated to large separations using a regression method which preserves the asymptotic characteristics of the space-time correlation (Li and Meroney, 1985). Integral scales were estimated by integrating over the extended correlation domain.

The space-time correlation function is plotted versus $x_i/(U_g T_{ii})$. The shear layer values for filtered turbulence are included on Figure 12 and compared with several sets of Eulerian space-time correlation data from other laboratory experiments. These experiments include data measured in another turbulent boundary layer; Frenkiel and Klebnoff, 1966), in grid turbulence corrected for energy decay (Comte-Bellot and Corrsin,1971), and in a nearly homogeneous turbulent shear flow (Harris et al., 1977).

Space-time correlation functions for an unfiltered turbulence are replotted against normalized time coordinates in Figures 13 through 15 for all three components of velocity fluctuations. Data are in good agreement with previous results for filtered turbulence. A universal shape for the Eulerian space-time correlation function seems to exist when presented in the non-dimensional coordinates. Such an empirical curve is superimposed over the data in the Figures 12 through 15.

REFERENCES

Atesmen, K.M., Baldwin, L.V. and Haberstroh, R.D., "The dispersion of matter in turbulent pipe flows, Trans. ASME, J. of Basic Engineering, Vol. 93, Series D., No. 4, 1971.

Baldwin, L.V. and Mickelsen, W.R., "Turbulent diffusion and anemometer measurements," Trans. ASCE, Vol. 128, pp. 1595-1627, 1963.

Baldwin, L.V. and Walsh, T.J., "Turbulent diffusion in the core of fully developed pipe flow." A.I.Ch.E.J., Vol. 7, pp. 53-61, 1961.

Blackwelder, R.F. and Kovasznay, L.S.G., "Time scales and correlations in a turbulent boundary layer," Phy. Fluids, Vol. 15, pp. 1545-1554, 1972.

Champagne, F.H., Harris, V.G. and Corrsin, S., "Experiments on nearly homogeneous turbulent shear flow," J. Fluid Mech., Vol. 41, pp. 81-139, 1970.

Comte-Bellot, G. and Corrsin, S., "Simple Eulerian time correlation of full and narrow-band velocity signals in grid-generated, isotropic turbulence," J. Fluid Mech., Vol. 48, pp. 273-337, 1971.

Counihan, J., "Adiabatic atmospheric boundary layer: A review and analysis of data from the period 1880-1972, Atmospheric Environment, Vol. 9, No. 10, pp. 871-905, 1975.

Favre, A.J., "Review on space-time correlations in turbulent fluids," Trans. ASME, J. Applied Mech., Vol. 32, pp. 241-257, 1965

Favre, A.J., Gaviglio, J.J. and Dumas, R.J.,

"Further space-time correlation of velocity in a turbulent boundary layer," J. Fluid Mech., Vol. 3, pp. 344-356, 1958.

Favre, A.J., Gaviglio, J.J., and Dumas, R.J., "Space-time double correlations and spectra in a turbulent boundary layer," J. Fluid Mech., Vol. 2, pp. 313-342, 1957.

Favre, A., Gaviglio, J. and Dumas, R., "Structure of velocity space-time correlations in a boundary layer," Phys. Fluids. Supplement, Vol. 10, pp. S138-S145, 1967.

Fisher, M.J. and Davies, P.O.A.L., "Correlation measurements in a non-frozen pattern of turbulence," J. Fluid Mech., Vol. 18, pp. 97-116, 1964.

Frenkiel, F.N. and Klebnoff, P.S., "Space-time correlations in turbulence," Dynamics of Fluid and Plasmas, S.I. Pai (editor), Academic Press, pp. 257-274, 1966.

Harris, V.G., Graham, J.A.H. and Corrsin, S., "Further experiments in nearly homogeneous turbulent shear flow," J. Fluid Mech., Vol. 81, pp. 657-687, 1977.

Li, W. W. and Meroney, R. N., "Estimation of Lagrangian time scale from laboratory measurements of lateral dispersion, Atmos. Environment, Vol. 18, pp. 1601-1611, 1984.

Li, W.W. and Meroney, R.N., "The estimation of atmospheric dispersion at nuclear power plants utilizing real time anemometer statistics." Technical Report for Nuclear Regulatory Commission, NUREG1CR-4072. Colorado State University, Fort Collins, Colorado, 215 pp., 1985.

Lumley, J.L. and Panofsky, H.A., The structure of atmospheric turbulence, John Wiley and Sons, Inc. 239 pp., 1964.

Plate, E. J. and Cermak, J. E., "Micrometeorological wind tunnel facility, description and characteristics. CER63EJP-JEC9, Colorado State University, Fort Collins, Colorado, 1963.

Teunissen, H.W., "Structure of mean winds and turbulence in the planetary boundary layer over rural terrain," Boundary-Layer Meterology, Vol. 19, pp. 187-221, 1980.

Table 1 Characteristics of the simulated atmospheric boundary layer, neutral

Table 2 Turbulent length scale of the neutral stratified boundary layer

(a) Integral length scales

z/δ	L_{11}	L_{12}	L_{21}	L_{22}	L_{31}	L_{32}
.044	19.5	2.54	--	--	2.10	.78
.22	26.9	4.69	5.22	5.14	4.00	2.35
.44	26.0	5.50	5.59	6.01	5.18	3.46

(b) Normalized integral length scales.

z/δ	$\frac{L_{21}}{L_{11}}$	$\frac{L_{12}}{L_{11}}$	$\frac{L_{21}}{L_{11}}$	$\frac{L_{22}}{L_{11}}$	$\frac{L_{31}}{L_{11}}$	$\frac{L_{32}}{L_{11}}$
.044	1	.13	--	--	.11	.040
.22	1	.17	.19	.19	.15	.087
.44	1	.21	.22	.23	.20	.13
Teunissen* (1980)	1	.18	.40	.22	.14	.027
Teunissen (1980)**	1	.19	.31	.23	.000	.060

* From correlation integral
** From exponential fit

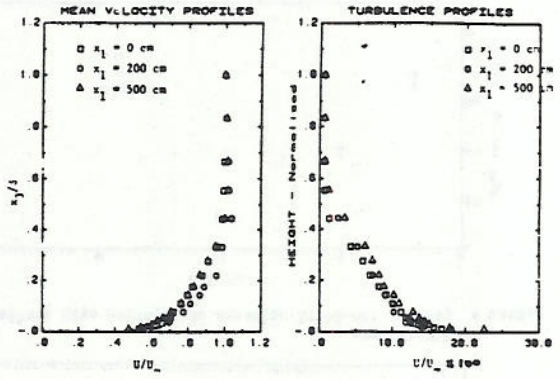

Figure 1 Mean velocity and turbulent intesity profiles for neutral stratified boundary layer at U_∞ = 200 cm/sec.

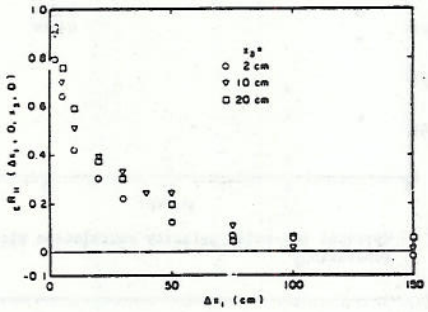

Figure 2 Longitudinal Eulerian space correlation

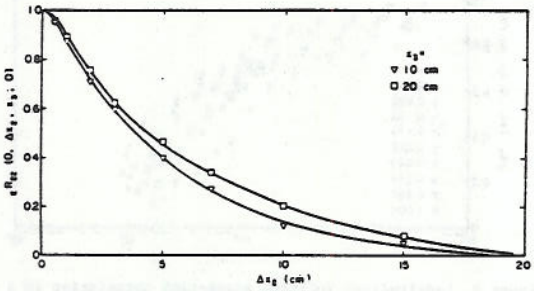

Figure 3 Lateral Eulerian space correlation

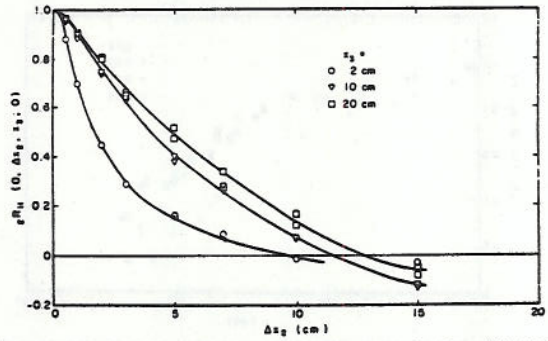

Figure 4 Longitudinal two-point velocity correlation with transverse separations

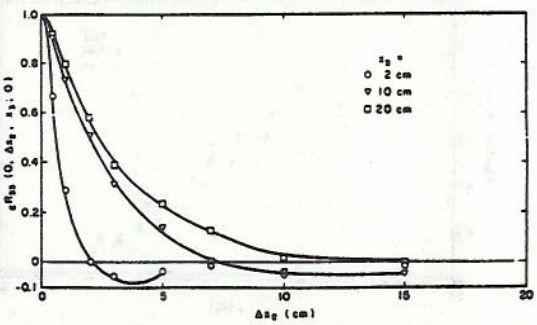

Figure 5 Vertical two-point velocity correlation with transverse separations

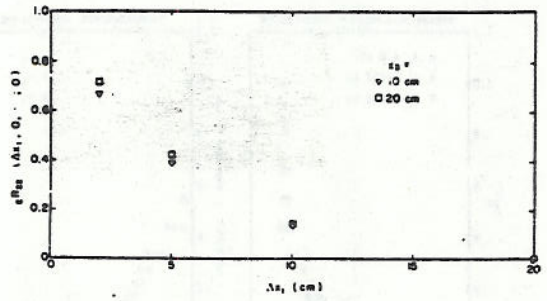

Figure 6 Lateral two-point velocity correlation with longitudinal separations

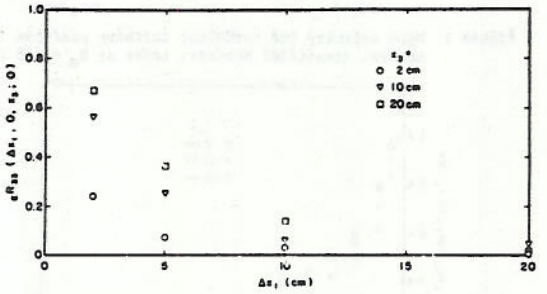

Figure 7 Vertical two-point velocity correlation with longitudinal separations

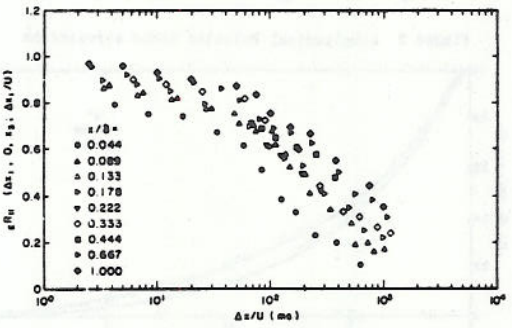

Figure 8 Longitudinal Eulerian space-time correlation in a neutral stratified boundary layer (filtered)

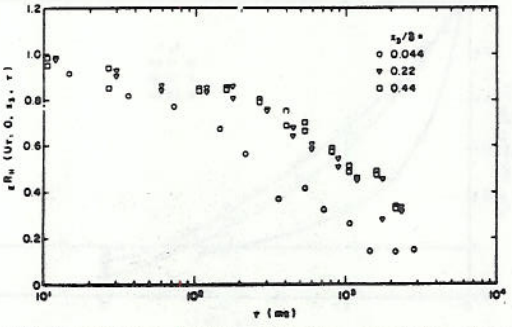

Figure 9 Longitudinal Eulerian space-time correlation in a neutral stratified boundary layer

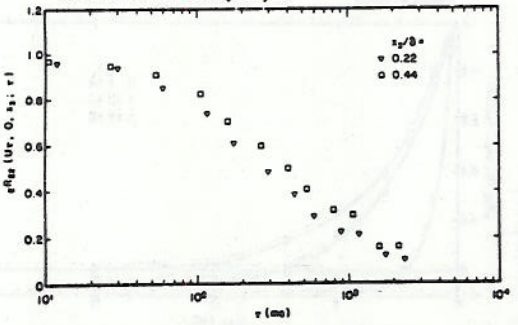

Figure 10 Transverse Eulerian space-time correlation in a neutral stratified boundary layer

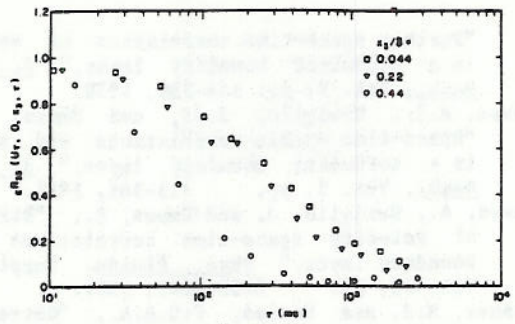

Figure 11 Vertical Eulerian space-time correlation in a neutral stratified boundary layer

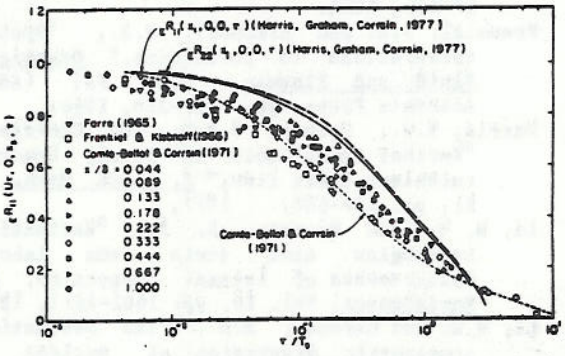

Figure 12 Normalized longitudinal space-time correlation in the boundary layer

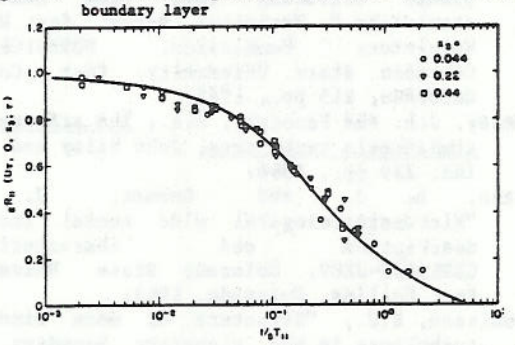

Figure 13 Normalized longitudinal space-time correlation in the boundary layer

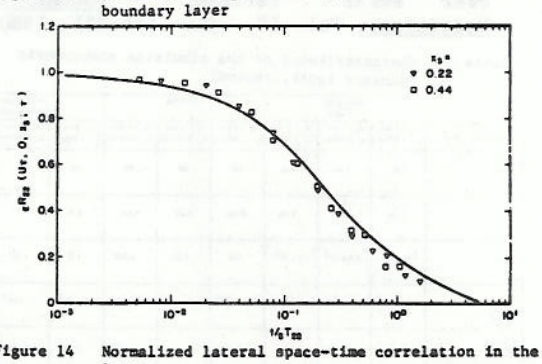

Figure 14 Normalized lateral space-time correlation in the boundary layer

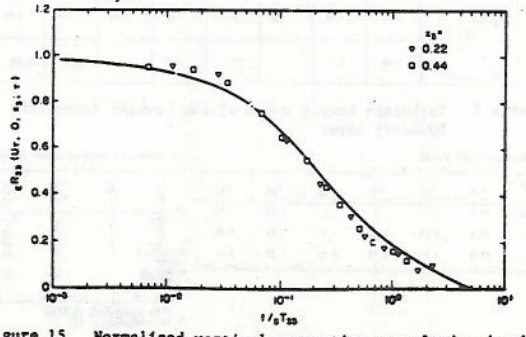

Figure 15 Normalized vertical space-time correlation in the boundary layer